OPTIMISATION OF WORKING PARAMETERS FOR SPOT FERTILISATION DEVICE WITH ECCENTRIC INTERMITTENT MECHANISM

1

偏心间歇式点施肥装置工作参数的优化

Ruihua ZHANG¹⁾, Xu ZHAO¹⁾, Jian WANG¹⁾, Wenjun WANG^{1,2,3*)}, Xiaomeng XIA^{1,2,3)}

School of Agricultural Engineering and Food Science, Shandong University of Technology, Zibo 255000, China.
 Institute of Modern Agricultural Equipment, Shandong University of Technology, Zibo 255000, China.
 Shandong Provincial Key Laboratory of Smart Agricultural Technology and Intelligent Farm Machinery Equipment for Field Crops, Zibo 255000, China.

Wenjun Wang, Tel: +86 15550326189; E-mail: wjwang2016@sdut.edu.cn, wjwang2016@163.com DOI: https://doi.org/10.35633/inmateh-77-27

Keywords: Precision fertilisation; Geneva mechanism; DEM-MBD; Full factorial experiment; Fertiliser discharge performance

ABSTRACT

To achieve precise fertilisation and improve fertiliser utilisation, an eccentric intermittent spot fertilisation device was designed in this study. The device can concentrate the continuous fertiliser flow from the fertiliser discharger into intermittently discharged fertiliser clusters, and accelerate the discharge of fertiliser into the fertiliser furrow through a Geneva mechanism. Full factorial experiments based on DEM-MBD coupled simulation show that both travel speed of implement and fertiliser discharge mass had a significant effect on the degree of dispersion and the coefficient of variation (CV) of fertiliser discharge. When the travel speed was 2.5 m/s and the fertiliser discharge mass was 6 g, the device had the best performance (degree of dispersion was 5.57 and the CV of fertiliser discharge was 3.27%). The results of the soil bin verification experiment indicate that the fertiliser pile length was 81.9 mm and the CV of fertiliser discharge was 4.30% under the optimum combination of working parameters. The absolute error between this result and the simulation result was 0.04 and 1.03%. This study shows that the device has better performance under the optimal working parameters.

摘要

为了实现精准施肥并提高肥料利用率,本研究设计了一种偏心间歇式点施肥装置。该装置可将排肥器连续输出的肥料流集中成间歇输出的肥料团,并通过槽轮机构加速肥料排入肥沟。基于 DEM-MBD 耦合仿真的全因子试验表明,机具行进速度和单次排肥量对肥料离散程度和排肥量变异系数均有显著影响。当行进速度为 2.5 m/s 且肥料排放量为 6 g 时,该装置表现最佳(离散度为 5.57,排肥量变异系数为 3.27%)。土槽验证试验结果表明,在最佳工作参数组合下,肥料堆长度为 81.9 mm,排肥量变异系数为 4.30%。该结果与仿真结果的绝对误差分别为 0.04 和 1.03%。本研究表明,偏心间歇点施肥装置在最佳参数下具有更优的性能。

INTRODUCTION

Spot application is a precise fertilisation technology based on the characteristics of crop root distribution, which achieves a concentrated supply of nutrients by applying fertilisers in a fixed point, quantitatively and precisely near the crop root system (*Yuan et al., 2018*). This type of fertilisation can significantly improve the fertiliser utilisation rate and reduce the amount of fertiliser applied, which achieves high crop yield and high quality and sustainable soil use (*Liu, 2017*).

In order to improve the applicability of the spot fertilisation device, the researchers designed the device as an indirect connection type. This type of spot fertilisation device achieves spot fertiliser application by installing a spot fertilisation device under the existing external groove wheel fertiliser applicator (*Liu et al., 2023*), which ensures the stability of obtaining fertiliser and the uniformity of the fertilisation mass (*Dun et al., 2025*). According to the principle of fertiliser discharge, indirect spot fertilisation devices are mainly classified into reciprocating and rotating types. Reciprocating spot fertilisation devices use devices such as flaps to control the opening and closing of the fertiliser discharge channel, thus achieving intermittent fertiliser discharge (*Gao et al., 2023; Zhang et al., 2018*).

¹ Ruihua Zhang, Master; Xu Zhao, Master; Jian Wang, Master; Wenjun Wang, Associate Professor; Xiaomeng Xia, Lecturer

However, the reciprocating motion has a lower working efficiency and the length of fertiliser is larger after it falls to the ground. The rotating spot fertilisation device rotates the fertiliser in the fertiliser filling zone to the fertiliser discharge zone through the rotation of the fertiliser discharge disc and then discharges the fertiliser at the fertiliser discharge zone (*Liu*, et al., 2018). The fertiliser discharge disc improves work efficiency of the device, but needs to be equipped with additional devices such as a fan to assist in discharging the fertiliser, which increases the complexity of the structure and the energy consumption (*Du et al.*, 2021). In this study, based on a rotating fertiliser discharge mechanism, the motion characteristics of the Geneva mechanism were utilised to impart a certain acceleration to the fertiliser clusters, eliminating the need for fans and thereby reducing fertiliser dispersion and structural complexity.

Wan et al. (2020) conducted field experiments at different travel speeds and concluded that the fertiliser discharge effect is best when the travel speed is 1.5 m/s. Du et al. (2022) designed a root-zone precision fertilisation device to analyse the fertiliser distribution length and CV of fertiliser discharge under different working parameters (fertiliser discharge mass, discharge height, travel speed). From the above analysis, it can be seen that the working parameters have a significant impact on the operating effect of the spot fertilisation device. The coupling of DEM and MBD can accurately reflect the mechanical properties and motion state of the system (Rodriguez et al., 2022). Zinkevičienė et al. (2021) established a simulation model of centrifugal spreader applying organic fertilisers to assess the transverse uniformity of the fertiliser in the field. Deng et al. (2024) simulated the process of under-membrane fertilisation to optimise the application of water and fertiliser by using a DEM-MBD coupled simulation. Dun et al. (2024) established a coupled model based on MBD-DEM and analysed the effects of working parameters on the uniformity coefficients of longitudinal and transverse fertilisation.

In summary, this study used a DEM-MBD coupled simulation method to investigate the impact of key working parameters (travel speed of the implement and single-dose fertiliser discharge mass) on the fertiliser discharge performance of the device, and identified the optimal combination of working parameters. Finally, the results of the simulation analyses were verified by soil bin experiments. This study reveals the relationship between the working parameters and the fertiliser discharge performance, which can provide a theoretical basis for optimising operational parameters.

MATERIALS AND METHODS

Overall structure and working principle

The structure of the seeder installed with eccentric intermittent spot fertilisation device is shown in Fig. 1(b). The spot fertilisation system mainly consists of fertiliser tank, external groove wheel fertiliser applicator, eccentric intermittent spot fertilisation device, fertiliser opener and so on. During the sowing operation, the tractor pulls the seeder forward through the four-bar linkage. The seeding opener creates the seed furrow, while the fertilizer opener forms the fertilizer furrow 5-8 cm below and to the side of the seed furrow. The maize precision seed meter then delivers the seeds into the seed furrow through the seed tube. The continuous fertilizer flow produced by the external groove wheel applicator is converted into discrete fertilizer clusters that fall into the fertilizer furrow under the action of the eccentric intermittent spot fertilization device. Subsequently, the press wheel refills the soil and covers the seeds, ensuring close contact between the seeds and the soil (*Ding et al.*, 2023).

The structure of the eccentric intermittent spot fertilisation device is shown in Fig. 1(a). The device is connected to the lower end of the external groove wheel fertiliser applicator through the fertiliser inlet pipe, the fertiliser output from the external groove wheel fertiliser applicator falls into the fertiliser filling zone through the fertiliser inlet pipe. To avoid crushing the fertiliser with the blades (4), which interferes with the stability of the fertiliser discharge mass, the operator can adjust the size of d according to the fertiliser size.

The continuous rotation of the motor is converted into intermittent movement of the rotor (5) through the Geneva mechanism, which in turn drives the intermittent rotation of the blades (4) mounted in the rotor (5). One end of the blade (4) is pressed against the surface of the cam (6) under the pressure of the blade spring (3), so that the other end maintains a certain gap d with the inner wall of the shell (7). When the spot fertilisation device is in operation, the fertiliser gradually concentrates into a motion layer during the rotation of the blade (4). The layers of fertiliser collide and merge under the driving of the blade (4), forming a complete fertiliser cluster in the fertiliser discharge zone. The fertiliser cluster is rapidly cast out from the fertiliser discharge zone under the effect of inertia and gravity, and falls into the fertiliser furrow under the guidance of the fertiliser discharge pipe.

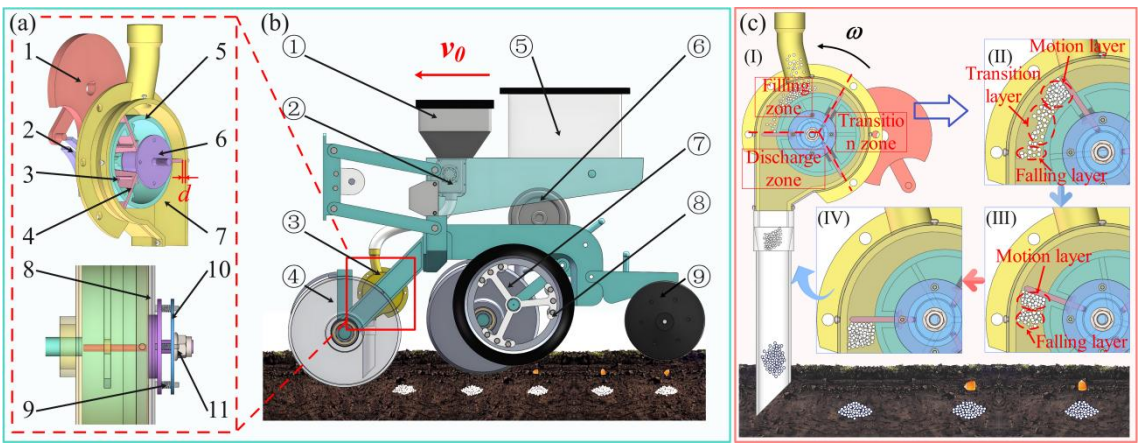


Fig. 1 - Structure of the eccentric intermittent fertilisation device and the process of fertiliser discharge

(a) Spot fertilisation device structure schematic, 1. Drive disk 2. Geneva wheel 3. Blade spring 4. Blade 5. Rotor 6. Cam 7. Fertiliser chamber shell 8. Shell cover 9. Compression spring 10. Barrier plate 11. Adjusting nut. (b) Overall structure of the seeder,

(1) Fertiliser tank (2). External groove wheel fertiliser applicator (3). Eccentric intermittent spot fertilisation device (4). Fertiliser opener

(5) Seed tank (6). Maize precision seed meter (7). Sowing opener (8). Depth control wheel (9). Press wheel. (c) Fertiliser application process of the spot fertilisation device, (1) Fertiliser filling stage, (1) Accelerated stage, (1) Decelerated stage, (1) Fertiliser discharge stage.

Simulation analysis of working parameters of spot fertilisation device

Simulation model and simulation parameters

The three-axis dimensions of 100 sample particles were measured using a vernier calliper, and the average fertiliser particle dimensions were 4.54 mm × 4.36 mm × 4.12 mm. From equation (1), the equivalent diameter and sphericity of the fertiliser particles, were 4.34 mm and 95.59%, respectively (Yuan et al., 2023).

$$D = \sqrt[3]{LWT}; \ \phi = \frac{D}{L}$$
 (1)

where: D is equivalent diameter of fertiliser particles, mm; φ is sphericity of fertiliser particles, %; L, W, T is length, width and height of fertiliser particles, mm.

Firstly, the coupling interface of DEM-MBD was configured, and the 3D model of the spot fertilisation device created by SolidWorks 2022 software was imported into RecurDyn 2023 software. Then the constraints and contacts between the components were set, and movement to the drive disc was added. The simulation time was set to 3 s and the Step was set to 800. All components were imported into EDEM 2021, then a fertiliser particle model was created. The fertiliser particle was set to be a single sphere with a diameter of 4.34 mm, generated according to a normal distribution, with a mean value of 1 and a standard deviation of 0.1. The surface of the fertiliser particles was regarded as non-adhesive, so the Hertz-Mindlin no-slip contact model was selected, and the fertiliser generation rate was set. The material of the spot fertilisation device is ABS plastic, and each simulation parameter is shown in Tables 1 and 2. The step time was set to 5.6×10-6 s in EDEM, and the data saving interval was 0.005 s (*Zhou et al., 2021*).

Simulation model parameters

Table 1

Item	Poisson's ratio	Shear modulus(Pa)	Density(kg/m³)
Fertiliser particle	0.25	1.8×10 ⁸	1800
Spot fertilisation device	0.5	1.77 x 10 ⁸	1180

Table 2

Model contact parameters

Item	Coefficient of restitution	Static friction coefficient	Rolling friction coefficient
Fertiliser - Fertiliser	0.25	0.39	0.14
Fertiliser - device	0.33	0.31	0.18

Experimental programme for full factorial experiment

Minitab 22 software was used to conduct a two-factor, three-level full factorial experimental design (Sezgin & Berkalp, 2018). The experimental factors and their level distributions are presented in Table 3. The number of blocks and replications were set to 1 and 2, respectively.

The experiments were carried out according to the specified running order, and each experimental group was repeated three times to minimize experimental error.

Experimental design scheme for the full factorial experiment

Table 3

Level —	Experiment factor				
Level —	Travel speed A(m/s)	Fertiliser discharge mass B(g)			
1	2.5	4			
2	3.0	6			
3	3.5	8			

As shown in Fig. 2, the start time of the fertilizer discharge stage was set to 0 s. When t < 0, the fertilizer was located in the filling zone. When $0 \le t < 0.01$, it was located in the discharge zone. The fertilizer was completely discharged from the spot fertilization device at approximately t = 0.01 s.

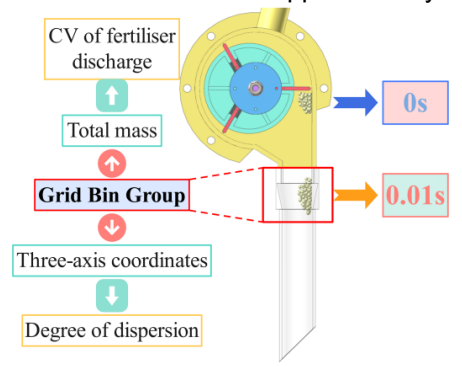


Fig. 2 - Fertiliser position and time node diagram in simulation analysis

The degree of dispersion and the CV of fertilizer discharge were used as evaluation indexes in the experiment, with the degree of dispersion quantified by the standard deviation. The standard deviation reflects the average deviation of data points from the central position. For a set of three-dimensional spatial points (x_i , y_i , z_i), a larger standard deviation indicates greater spatial dispersion. A Grid Bin Group was added at the outlet of the spot fertilization device in the EDEM post-processing interface (He et al., 2019). After completing the simulation, the total mass and three-axis coordinates of the fertilizer particles within the Grid Bin Group were exported. Each simulation collected 20 sets of fertilizer particle data, and the degree of dispersion and the CV of fertilizer discharge were calculated according to Eqs. (2) and (3).

$$S = \sqrt{\frac{\sum_{i=1}^{k} (\sqrt{x_i^2 + y_i^2 + z_i^2} - \frac{\sum_{i=1}^{k} \sqrt{x_i^2 + y_i^2 + z_i^2}}{k})^2}{k}}$$

$$q = \frac{\sqrt{\frac{1}{j} \sum_{i=1}^{j} (m_i - m_c)^2}}{m_c} \times 100\%$$
(3)

$$q = \frac{\sqrt{\frac{1}{j} \sum_{i=1}^{j} (m_i - m_c)^2}}{m_c} \times 100\%$$
 (3)

where: S is degree of fertiliser dispersion; x_i , y_i , z_i is distance of fertiliser particles in x,y,z-axis direction, mm; q is CV of fertiliser discharge, %; m_c is average fertiliser discharge, g; m_i is actual discharge, g.

Soil bin verification experiment

In order to validate the simulation analysis results, the soil bin experiment was conducted in the modern agricultural equipment laboratory of Shandong University of Technology (118°00'19.56"E, 36°48'18.18"N). The eccentric intermittent spot fertilisation system bench was implemented and assembled, and the experiment environment and experiment equipment were installed as shown in Fig. 3(a).

The factors and levels in the verification experiment are the same as those in the full factorial experiment. The fertiliser pile length, the CV of pile length, the CV of fertiliser spacing and the CV of fertiliser discharge were selected to evaluate the operational performance of the eccentric intermittent spot fertilisation device. Before the experiment, a furrow opener was used to create an 80 mm deep fertiliser furrow. After each experiment, 20 piles of fertiliser were continuously selected for measurement in the velocity stability zone. Each group of experiments was repeated three times and the average value was taken.

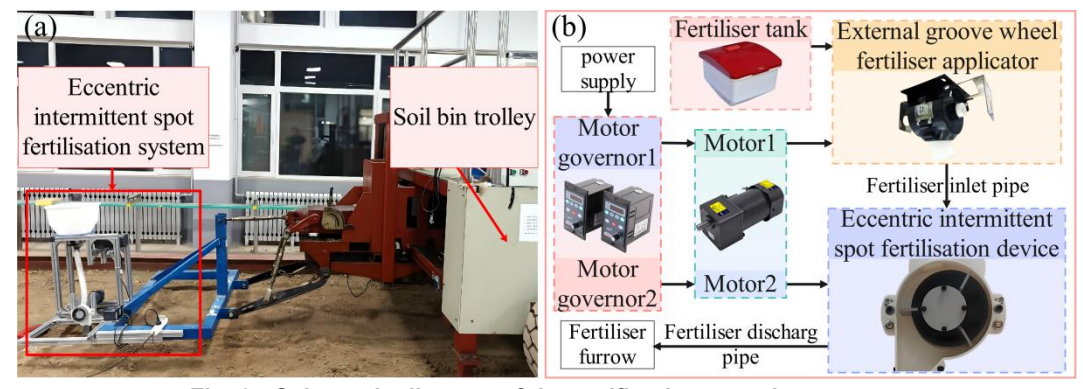


Fig. 3 - Schematic diagram of the verification experiment setup

(a) Experimental environment and equipment; (b) Operating principle of the spot fertilisation system.

The experimental results were obtained as shown in Fig. 6. The majority of fertiliser particles were enclosed by the smallest-area ellipse, and the length of its major axis was defined as the fertiliser pile length. The distance between the centres of two adjacent ellipses represented the fertiliser spacing. An electronic scale was then used to measure the weight of each fertiliser pile. The expressions for the CV of fertiliser pile length, fertiliser spacing, and fertiliser discharge are given in Eqs. (4), (5), and (3), respectively.

$$C = \frac{\sqrt{\frac{1}{j} \sum_{e=1}^{j} (l_e - l_a)^2}}{l_a} \times 100\%$$
 (4)

$$p = \frac{\sqrt{\frac{1}{j} \sum_{i=1}^{j} (L_i - L_a)^2}}{L_a} \times 100\%$$
 (5)

where: C is CV of fertiliser pile length, %; l_a is average fertiliser pile length, mm; l_e is actual fertiliser pile length, mm; p is CV of fertiliser spacing, %; L_a is average fertiliser spacing, mm; L_i is actual spacing, mm.

The RMSE was selected to evaluate the error between the actual operating effect of the spot fertilisation device and the simulation results, as shown in equation (6). There is an extremely strong positive correlation between the degree of dispersion and fertiliser pile length. To compare and analyse these two sets of data, min-max normalization was applied to both datasets to eliminate dimensional and scale effects.

RMSE =
$$\sqrt{\frac{\sum_{i=1}^{n} (y_i - y_e)^2}{n}}$$
 (6)

where: RMSE is root mean square error; y_t is verification experiment data; y_e is simulation analysis data.

RESULTS

Simulation results and analysis

Experiment results and analysis of variance

The combinations and experiment results of the experiment are shown in Table 4. A variance analysis (ANOVA) of the experimental results was performed using Minitab 22 software, the results of the analysis of the degree of fertilisers dispersion and the CV of fertiliser discharge are shown in Table 5.

Experiment results for each group of experiments

Table 4

Standard sequence	Running sequence	Point type	Block	Travel speed A (m/s)	Fertiliser discharge mass <i>B</i> (g)	Degree of dispersion Y ₁	CV of fertiliser discharge Y ₂ (%)
3	1	1	1	2.5	5	5.36	4.93
12	2	1	1	2.5	5	5.63	4.82
11	3	1	1	2.5	4	5.59	3.41
13	4	1	1	3	3	5.49	3.98
9	5	1	1	3.5	5	6.82	9.30
2	6	1	1	2.5	4	5.55	3.12
6	7	1	1	3	5	5.98	6.78
18	8	1	1	3.5	5	6.59	8.45

Standard sequence	Running sequence	Point type	Block	Travel speed A (m/s)	Fertiliser discharge mass <i>B</i> (g)	Degree of dispersion Y ₁	CV of fertiliser discharge Y ₂ (%)
8	9	1	1	3.5	4	6.55	7.20
15	10	1	1	3	5	6.02	6.92
1	11	1	1	2.5	3	5.67	3.05
7	12	1	1	3.5	3	6.11	6.50
16	13	1	1	3.5	3	6.24	6.75
17	14	1	1	3.5	4	6.62	7.10
10	15	1	1	2.5	3	5.68	3.15
4	16	1	1	3	3	5.57	3.54
5	17	1	1	3	4	5.28	4.69
14	18	1	1	3	4	5.42	4.21

Table 5

ANO	VA	tab	le
-----	----	-----	----

Indicators	Source	Degree of freedom	Adj SS	Adj MS	F-value	P-value
	Model 1	8	3.93160	0.49145	50.01	0.000
	Linear	4	3.39967	0.84992	86.48	0.000
	Α	2	3.13943	1.56972	159.72	0.000
Y_1	В	2	0.26023	0.13012	13.24	0.002
	$A \times B$	4	0.53193	0.13298	13.53	0.001
	Error	9	0.08845	0.00983		
	Total	17	4.02005			
	Model 2	8	64.8872	8.1109	108.56	0.000
	Linear	4	63.9570	15.9892	214.01	0.000
	Α	2	44.9752	22.4876	300.99	0.000
Y_2	В	2	18.9817	9.4909	127.03	0.000
	$A \times B$	4	0.9302	0.2325	3.11	0.073
	Error	9	0.6724	0.0747		
	Total	17	65.5596			

From the above ANOVA table, it can be seen that the P-value of both models is less than 0.05, which indicates that the factor analysis model established for this trial is valid. For the degree of dispersion, both travel speed and fertiliser discharge mass had a significant effect (p < 0.05), and the two-factor interaction was also significant (p < 0.05). The standardised effects from largest to smallest were A > AB > B. The regression model fit well with S = 0.099, R² = 97.80%. For the CV of fertiliser discharge, both travel speed and fertiliser discharge mass had a significant effect (p < 0.05). However, the two-factor interaction was not significant (p > 0.05). The standardised effects from largest to smallest are A > B > AB. The model has S = 0.273, R² = 98.97%. The factorial plots for the two experimental indicators are shown in the Figure 4.

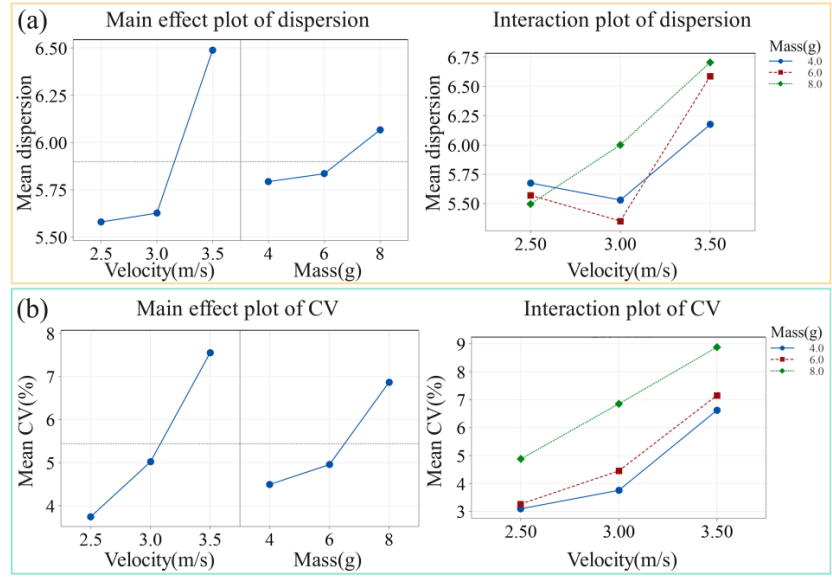


Fig. 4 - Factorial plots of degree of dispersion and CV of fertiliser discharge (a) Factorial plot for degree of dispersion. (b) Factorial plot for CV of fertiliser discharge.

Minimising the degree of dispersion and minimising the CV of fertiliser discharge are taken as the optimum conditions (*Tang et al., 2023*). The constraint ranges of the objective function and working parameters are shown in Eq. (7). Using Minitab 22 software to solve the parameter optimisation, when the travel speed is 2.5 m/s and the single-dose fertiliser discharge mass is 6 g, the degree of dispersion is 5.57 and the CV of fertiliser discharge is 3.27%.

$$\begin{cases}
\min Y_1(A, B) \\
\min Y_2(A, B)
\end{cases} \quad s.t. \begin{cases}
2.5 \text{m/s} \le A \le 3.5 \text{m/s} \\
4g \le B \le 8g
\end{cases} \tag{7}$$

Analysis of the influence of working parameters

(1) Degree of fertiliser dispersion

Figure 5(a) demonstrates a negative correlation between the degree of dispersion and discharge mass at low speeds, shifting to a positive correlation at higher speeds. This discrepancy with *Li et al.* (2024) may arise from incomplete particle collisions and cluster merging with small discharge mass at low speed, increasing dispersion. Larger discharge masses promote complete merging, reducing dispersion, while higher speeds enhance centrifugal forces, where increased mass destabilises fertiliser flow and amplifies dispersion.

With small discharge masses, the dispersion degree initially decreases then increases with travel speed, while showing a consistent positive correlation with large masses. This partial inconsistency with *Liu et al.* (2023) may stem from: with small masses, increased speed initially accelerates fertiliser clusters, shortening discharge time and reducing dispersion, but higher speeds subsequently destabilize fertiliser flow. With large masses, fertiliser accumulation at the inlet promotes fertiliser backflow, and rising speeds progressively destabilise flow to increase dispersion.

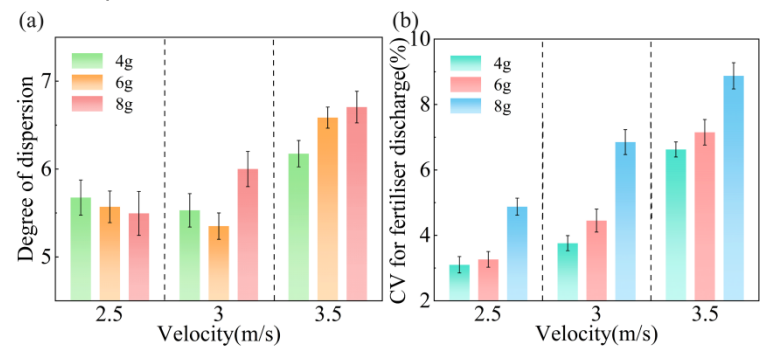


Fig. 5 - Changes of experiment indexes under different working parameters
(a) Variation in degree of dispersion under different travel speeds and fertiliser discharge masses.
(b) Variation in CV of fertiliser discharge under different travel speeds and fertiliser discharge masses.

(2) CV of fertiliser discharge

Figure 5(b) demonstrates that at a constant travel speed, the CV of fertiliser discharge increases with discharge mass, contradicting *Li et al.* (2024). This discrepancy may stem from increased fertiliser accumulation thickness and centrifugal force at larger discharge masses, intensifying backflow phenomena.

At a constant discharge mass, the CV of fertiliser discharge increases with travel speed, consistent with *Du et al. (2021)*. This likely results from increased rotor speed and centrifugal force at higher travel speeds, which intensify fertiliser flow interference and consequently elevate discharge variability.

Verification experiment results and analysis



Fig. 6 - Results and measurement methods of the verification experiment

Fig. 7(a) shows that under conditions of 2.5-3.5 m/s and 4-8 g, the fertiliser pile length was 73.2-120.5 mm (normalised to 0-1), with a maximum absolute error of 0.07 and an RMSE of 0.05. At a constant discharge mass, the pile length initially decreased then increased with speed. Lower speeds showed inverse proportionality between pile length and discharge mass, while higher speeds demonstrated direct proportionality.

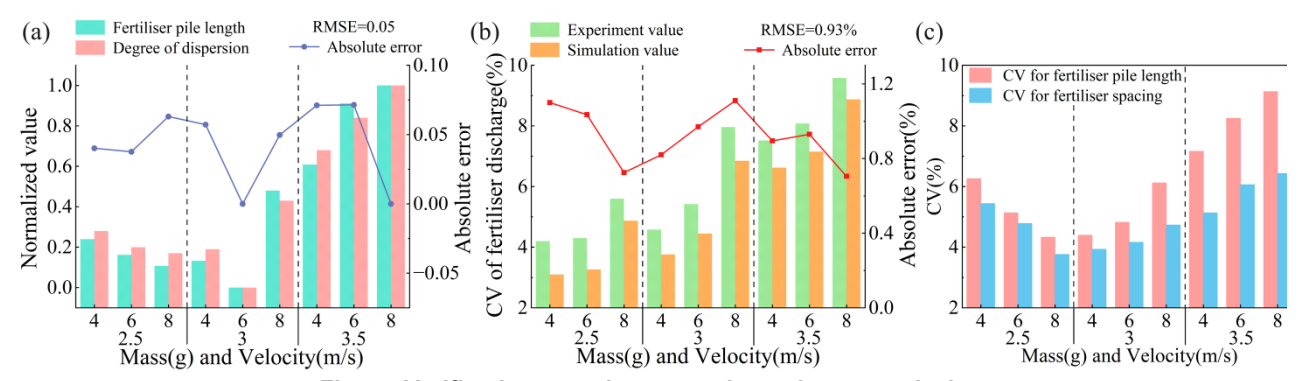


Fig. 7 - Verification experiment results and error analysis

(a) Error analysis between degree of dispersion and fertiliser pile length; (b) Error analysis of the CV of fertiliser discharge, (c) changes in experimental indexes under different fertiliser discharge masses and travel speeds.

Figure 7(b) shows that under conditions of 2.5-3.5 m/s and 4-8 g, the CV of fertiliser discharge was 4.20%-9.58%, with a maximum absolute error of 1.11% and an RMSE of 0.93%. The CV increased with higher discharge mass or travel speed, matching simulation trends and confirming model reliability.

In addition, Figure 7(c) shows that under the experimental conditions, the CVs of fertiliser pile length and spacing were 4.33%-9.13% and 3.76%-6.43%, respectively. At smaller discharge mass, these CVs initially decreased and then increased with speed, while a larger mass showed gradual increases. The CVs exhibited inverse proportionality to discharge mass at low speeds but direct proportionality at high speeds. In conclusion, the eccentric intermittent spot fertilisation device had good operational performance.

CONCLUSIONS

This study designed an eccentric intermittent spot fertilisation device and investigated the influence of key working parameters on fertiliser discharge performance through DEM-MBD simulations and soil bin experiments. The main conclusions are as follows:

- (1) ANOVA results showed that travel speed and discharge mass significantly affected the degree of dispersion and the CV of discharge (P < 0.05). Their interaction had a significant effect on dispersion (P < 0.05) but not on CV (P > 0.05).
- (2) Simulation analysis showed that the degree of dispersion was minimal at 3 m/s and 6 g (5.35) and maximal at 3.5 m/s and 8 g (6.71). The CV of discharge was lowest at 2.5 m/s and 4 g (3.10%) and highest at 3.5 m/s and 8 g (8.87%). The optimal parameters were determined to be a travel speed of 2.5 m/s and a discharge mass of 6 g.
- (3) Soil bin experiment demonstrated that at a travel speed of 2.5-3.5 m/s and a discharge mass of 4-8 g, the fertiliser pile length was 73.2-120.5 mm (max absolute error: 0.07, RMSE: 0.05), and the CV of discharge was 4.20%-9.58% (max absolute error: 1.11%, RMSE: 0.93%). Under optimal parameters (2.5 m/s, 6 g), the pile length was 81.9 mm (max absolute error: 0.04%), the CV of discharge was 4.30% (max absolute error: 1.03%). Other experimental indicators included a CV of pile length of 4.33%-9.13% and a CV of spacing of 3.76%-6.43%. The spot fertilisation device performed well and met the operational requirements for fertilisation.

ACKNOWLEDGEMENT

This work was supported by the Natural Science Foundation of Shandong Province (ZR2024QE004, ZR2023QF143, ZR2023QE198), High-quality Development Project for the Ministry of Industry and Information (2023ZY02009), Youth Innovation Team Development Plan for Higher Education Institutions in Shandong Province (2022KJ225), National Natural Science Foundation of China (52405280).

REFERENCES

- [1] Deng, H., Dai, F., Shi, R., Song, X., Zhao, W., & Pan, H. (2024). Simulation of full-film double-row furrow roller hole fertiliser application based on DEM-MBD coupling and research on its water and fertiliser transport law. *Biosystems Engineering*, 239, 190-206. https://doi.org/10.1016/j.biosystemseng.2024.02.007
- [2] Ding, Y., Yang, L., He, X., Cui, T., Qi, B., Zhang, W., Xie, C., Du, Z., Li, Y., & Zhang, D. (2023). Development and performance evaluation of an automatic section control system for corn precision planters. *Computers and Electronics in Agriculture*, 206, 107670. https://doi.org/10.1016/j.compag.2023.107670
- [3] Du, X., Liu, C., Jiang, M., Yuan, H., Dai, L., & Li, F. (2021). Design and experiment of inclined trapezoidal hole fertilizer point-applied discharging device (倾斜梯形孔式穴施肥排肥器设计与试验). *Transactions of the Chinese Society for Agricultural Machinery*, 52(9), 43-53. https://doi.org/10.6041/j.issn.1000-1298.2021.09.005
- [4] Du, X., Liu, C., Jiang, M., & Yuan, H. (2022). Design and development of fertilizer point-applied device in root-zone. *Applied Engineering in Agriculture*, 38(3), 559-571. https://doi.org/10.13031/aea.14846
- [5] Dun, G., Ma, C., Ji, X., Li, H., Cheng, H., Sun, H., & Zhang, C. (2025). Optimization design and test of interactive anti-stick gear fertilizer discharger for pineapple, *INMATEH Agricultural Engineering*, 76(2), 461-474. https://doi.org/10.35633/inmateh-76-39
- [6] Dun, G., Sheng, Q., Ji, X., Li, X., Wei, Y., Gao, S., & Zhang, C. (2024). Optimization of and experimentation with a bifurcated swing tube strip fertilizer spreading device based on MBD-DEM coupling. *Frontiers in Plant Science*, 15, 1456173. https://doi.org/10.3389/fpls.2024.1456173
- [7] Gao, J., Zhang, F., Zhang, J., Zhou, H., & Yuan, T. (2023). Development and field performance evaluation of hole-fertilizing planter and dynamic alignment control system for precision planting of corn. *Precision Agriculture*, 24(4), 1241-1260. https://doi.org/10.1007/s11119-023-09988-6
- [8] He, B., Qi, J., Meng, H., Lin, Y., Zhou, X., & Zhao, W. (2019). Performance analysis and parameter optimization of diversion device of ditcher based on EDEM (基于 EDEM 的开沟机导流装置性能分析及参数优化). Journal of Chinese Agricultural Mechanization, 40(10), 25-29+41. https://doi.org/10.13733/j.jcam.issn.2095-5553.2019.10.06
- [9] Li, G., Su, X., Zhou, X., Zhang, X., Wang, Q., & Wang, C. (2024). Design and experiment of pneumatic assisted hole fertilization targeting seed position device (气力辅助式对种穴施肥装置设计与试验). *Transactions of the Chinese Society for Agricultural Machinery*, 55(12), 191-200. https://doi.org/10.6041/j.issn.1000-1298.2024.12.017
- [10] Liu, Q. (2017). Spatio-temporal changes of fertilization intensity and environmental safety threshold in China (中国化肥施用强度及环境安全阈值时空变化). *Transactions of the Chinese Society of Agricultural Engineering*, 33(6), 214-221. https://doi.org/10.11975/j.issn.1002-6819.2017.06.028
- [11] Liu, Z., Wang, Q., Liu, C., Li, H., He, J., & Liu, J. (2018). Design and experiment of precision hole-fertilizing apparatus with notched plate (腔盘式精量穴施肥装置设计与试验). *Transactions of the Chinese Society for Agricultural Machinery*, 49(10), 137-144. https://doi.org/10.6041/j.issn.1000-1298.2018.10.015
- [12] Liu, Z., Wang, X., Li, S., Huang, Y., Yan, X., & Zhao, H. (2023). Design of maize automatic hole fertilization system targeting at seed based on planetary gear train (基于行星轮系的玉米穴施肥自动对种系统设计与试验). *Transactions of the Chinese Society for Agricultural Machinery*, 54(3), 60-67. https://doi.org/10.6041/j.issn.1000-1298.2023.03.006
- [13] Rodriguez, V. A., Barrios, G. K.P., Bueno, G., & Tavares, L. M. (2022). Coupled DEM-MBD-PRM simulations of high-pressure grinding rolls. Part 1: Calibration and validation in pilot-scale. *Minerals Engineering*, 177, 107389. https://doi.org/10.1016/j.mineng.2021.107389
- [14] Sezgin, H., & Berkalp, O. B. (2018). Analysis of the effects of fabric reinforcement parameters on the mechanical properties of textile-based hybrid composites by full factorial experimental design method. *Journal of Industrial Textiles*, 48(3), 580-598. https://doi.org/10.1177/1528083717740764
- [15] Tang, H., Xu, F., Guan, T., Xu, C., & Wang, J. (2023). Design and experiment of a pneumatic type of high-speed maize precision seed metering device. *Computers and Electronics in Agriculture*, 211, 107997. https://doi.org/10.1016/j.compag.2023.107997

- [16] Wan, L., Xie, D., Li, Y., & Chen, L. (2020). Design and experiment of roller hole fertilizer application between corn rows (玉米行间滚轮式穴施排肥器设计与试验). *Transactions of the Chinese Society for Agricultural Machinery*, 51(11), 64-73. https://doi.org/10.6041/j.issn.1000-1298.2020.11.007
- [17] Yuan, F., Yu, H., Wang, L., Shi, Y., Wang, X., & Liu, H. (2023). Parameter Calibration and Systematic experiment of a Discrete Element Model (DEM) for Compound Fertilizer Particles in a Mechanized Variable-Rate Application. *Agronomy*, 13(3), 706. https://doi.org/10.3390/agronomy13030706
- [18] Yuan, W., Li, K., Jin, C., Hu, M., & Zhang, W. (2018). Design and experiment of hill placement fertilizer applicator (穴施肥排肥器设计与试验). *Journal of Agricultural Mechanization Research*, 40(1), 145-149+165. https://doi.org/10.13427/j.cnki.njyi.2018.01.027
- [19] Zhang, J., Liu, H., Gao, J., Lin, Z., & Chen, Y. (2018). Simulation and test of corn layer alignment position hole fertilization seeder based on SPH (玉米分层正位穴施肥精播机 SPH 仿真与试验). *Transactions of the Chinese Society for Agricultural Machinery*, 49(9), 66-72. https://doi.org/10.6041/j.issn.1000-1298.2018.09.007
- [20] Zhou, L., Yu, J., Liang, L., Wang, Y., Yu, Y., Yan, D., Sun, K., & Liang, P. (2021). DEM Parameter Calibration of Maize Seeds and the Effect of Rolling Friction. *Processes*, 9(6), 914. https://doi.org/10.3390/PR9060914
- [21] Zinkevičienė, R., Jotautienė, E., Juostas, A., Comparetti, A., & Vaiciukevičius, E. (2021). Simulation of Granular Organic Fertilizer Application by Centrifugal Spreader. *Agronomy*, 11(2), 247. https://doi.org/10.3390/agronomy11020247